Biochimica et Biophysica Acta 1798 (2010) 87–93

Contents lists available at ScienceDirect

Biochimica et Biophysica Acta

journal homepage: www.elsevier.com/locate/bbamem

NMR dynamics and antibody recognition of the meningococcal lipidated outer membrane protein LP2086 in micellar solution

Alessandro Mascioni [a], Franklin J. Moy [a], Lisa K. McNeil [b], Ellen Murphy [b], Breagh E. Bentley [b], Rosaria Camarda [b], Deborah A. Dilts [b], Pamela S. Fink [b], Viktoria Gusarova [b], Susan K. Hoiseth [b], Karl Malakian [a], Terri Mininni [b], Elena Novikova [b], Shuo Lin [b], Scott Sigethy [b], Gary W. Zlotnick [b,*], Désirée H.H. Tsao [a,*]

[a] Wyeth Research, Structural Biology and Computational Chemistry, 200 Cambridge Park Drive, Cambridge, MA 02140, USA
[b] Wyeth Vaccines Research, 401 North Middletown Road, Pearl River, NY 10965, USA

ARTICLE INFO

Article history:
Received 20 April 2009
Received in revised form 24 September 2009
Accepted 29 September 2009
Available online 14 October 2009

Keywords:
Outer membrane protein
Detergent micelle
Lipoprotein
Neisseria meningitidis
LP2086
Factor H binding protein
NMR spectroscopy
Structure
Dynamics
Membrane topology

ABSTRACT

Neisseria meningitidis is a major cause of meningitis. Although protective vaccination is available against some pathogenic serogroups, serogroup B meningococci have been a challenge for vaccinologists. A family of outer membrane lipoproteins, LP2086 (or factor H binding proteins, fHbp), has been shown to elicit bactericidal antibodies and is currently part of a cocktail vaccine candidate. The NMR structure of the variant LP2086-B01 in micellar solution provided insights on the topology of this family of proteins on the biological membrane. Based on flow cytometry experiments on whole meningococcal cells, binding experiments with monoclonal antibodies, and the NMR structure in micellar solution, we previously proposed that LP2086-B01 anchors the outer bacterial membrane through its lipidated N-terminal cysteine, while a flexible 20 residue linker positions the protein above the layer of lipo-oligosaccharides that surrounds the bacteria. This topology was suggested to increase the antigen exposure to the immune system. In the present work, using micellar solution as a membrane mimicking system, we characterized the backbone dynamics of the variant LP2086-B01 in both its lipidated and unlipidated forms. In addition, binding experiments with a Fab fragment derived from the monoclonal MN86-1042-2 were also performed. Our data suggests that due to the length and flexibility of the N-terminal linker, the antigen is not in contact with the micelle, thus making both N- and C-domains highly available to the host immune system. This dynamic model, combined with the binding data obtained with MN86-1042-2, supports our previously proposed arrangement that LP2086-B01 exposes one face to the extracellular space. Binding of MN86-1042-2 antibody shows that the N-domain is the primary target of this monoclonal, providing further indication that this domain is immunologically important for this family of proteins.

1. Introduction

Meningitis caused by the bacterium *Neisseria meningitidis* results in significant mortality and morbidity in humans. Of the five bacterial serogroups associated with the disease (A, B, C, Y and W135), successful preventive vaccination has been achieved for serogroups A, C, Y and W135, through the use of capsular polysaccharides conjugated to proteins [1]. In spite of the fact that serogroup B is responsible for 80% of the meningococcal diseases in Europe and 50% in the United States, a preventive vaccine against serogroup B is still missing [1–27]. The use of a glycoconjugate approach for serogroup B vaccination is hampered by the close structural similarity between the bacterial capsular polysaccharides and the sialic acid surface of developing human brain [3]. As a consequence, vaccine development for serogroup B has focused on the use of immunogenic outer membrane proteins. Initial attempts to achieve immunization against this serogroup using the integral membrane protein porin A (PorA) achieved only partial success. This was due to the high degree of sequence diversity of the PorA family across different meningococcal strains, which would require a difficult multivalent approach [28].

One relevant factor affecting the immunogenic properties of outer membrane proteins is their degree of exposure to the extracellular space. In the case of PorA for example, anti-porin bactericidal antibodies recognize only a few surface exposed loops that emerge from the surface of the outer membrane [4]. Among the factors affecting the exposure of meningococcal antigens is the presence of a

Abbreviations: fHBP, factor H binging protein; PorA, porin A; PorB, porin B; rLP2086, recombinant lipidated P2086; rP2086, recombinant non-lipidated P2086; rLP2086-B01, recombinant lipidated LP2086 variant B01; LOS, lipo-oligosaccharides; LPS, lipopolysaccharides; mAb, monoclonal antibody

* Corresponding authors. D.H.H. Tsao is to be contacted at fax: +1 617 665 5682.
E-mail addresses: zlotnig@wyeth.com (G.W. Zlotnick), dtsao@wyeth.com (D.H.H. Tsao).

0005-2736/$ – see front matter © 2009 Elsevier B.V. All rights reserved.
doi:10.1016/j.bbamem.2009.09.021

layer of lipopolysaccharides (LPS) that surrounds the outer membrane. In the case of porin B (PorB), it was shown that membrane-bound lipopolysaccharides with different chain lengths were able to shield PorB epitopes from the antibodies, reducing the efficacy of this class of proteins as vaccine candidate [5].

Recently, a new family of meningococcal outer membrane lipoproteins, LP2086 (also known as factor H binding protein, fHBP, or GNA1870), was found to induce bactericidal antibodies, and is presently being tested in humans as potential vaccine candidate against serogroup B meningococci [6]. Based on their genetic sequence, members of the LP2086 family were divided into two subfamilies, subfamily A and B [5,7]. The structure of the variant LP2086-B01 (PDB entry: 2KDY; Genbank accession number: AY330406) in micellar solution revealed a fold consisting of three regions. Two structured domains (the N-domain spanning residues 21–140, and the C-domain spanning residues 141–261), and a 20 residue N-terminal flexible chain (spanning residues 1–20), which anchors the protein to the membrane through a lipid moiety at residue 1 (tripalmitoyl-S-glycerol-cysteine) [8,9]. The N-terminal chain was suggested to act as a flexible spacer that separates the protein from the membrane surface and accommodates the layer of lipo-oligosaccharides (LOS) that surround the outer membrane of the bacteria. A topological model of the protein in the membrane was suggested based on binding experiments with monoclonal antibodies (mAb), and flow cytometry experiments on whole meningococcal cells [8]. LP2086-B01 was proposed to anchor the outer surface of the bacteria with one face of the protein oriented toward the extracellular space, while the opposite region connecting the N-terminal chain to the main fold faces toward the membrane surface [8].

In addition to steric effects that may come into play with the membrane and the LOS, the dynamic properties of membrane bound antigen may also play an important role in antibody–antigen recognition. In particular, lipidated membrane proteins embedded or seating on the surface of the lipo-oligosaccharides can experience restricted tumbling motion which makes certain regions of the protein inaccessible to the immune system.

As a first step towards characterizing the dynamic properties of LP2086-B01 in a system that mimics the biological membrane, we studied the backbone dynamics of the lipidated variant LP2086-B01 in micellar solution. Detergent micelles have been extensively used as membrane mimicking systems for the study of membrane proteins by solution NMR spectroscopy [10,11]. Similarly to biological membranes, these systems provide a hydrophobic core that accommodates hydrophobic regions of the protein, combined to a surface of charged head-groups that mimics the phosphate layer of the membrane.

In the present work, we have compared the dynamic properties of the lipidated LP2086-B01 with the non-lipidated free protein in solution. Our data shows that for the protein–micelle complex the R_2 relaxation rates increase with respect to the protein in the detergent-free sample. However, the magnitude of the increase in R_2 is not consistent with the substantially higher molecular weight of the protein–micelle complex. Based on the aggregation number, and the molecular weight of the detergent, a doubling in the molecular weight of the protein–micelle complex with respect to the micelle-free protein is estimated. Our NMR data on the other hand shows only minor changes in peak widths for LP2086-B01 in micellar solution. Since the protein is bound to the micelle through a 20 residue flexible N-terminal chain, and NOEs with the detergent are observed only for the first two residues of the unstructured N-terminus, we concluded that the main fold of the protein is not in contact with the micelle. We propose that the changes observed in the dynamic properties of the micelle-bound protein arise from motional restrictions imposed by the micelle-bound N-terminal chain which hamper the protein from tumbling istropically. The implications of these motional restrictions in antibody binding and the possible role of the lipo-oligosaccharides layer are discussed.

2. Materials and methods

2.1. Protein expression and purification

Expression and purification of lipidated rLP2086-B01 was performed as reported [6]. ^{15}N labeled rP2086-B01 was expressed from a pET9a vector, transformed in *E. coli* BLR(DE3)pLysS [6]. For the perdeuterated protein, cells were grown in minimum media containing 50 μg kanamycin in 99% D_2O, and enriched with 2 g/L ^{15}N-ammonium sulfate (Cambridge Isotope Laboratories). Expression was performed at 37 °C for 14 h after induction with 1 mM isopropyl β-D-thiogalactopyranoside (IPTG).

2.2. Production of Fab fragment from monoclonal antibodies

Fab fragments were obtained through papain digestion of monoclonal MN86-1042-2. Full length MN86-1042-2 antibody was dialyzed for 4 h in 20 mM phosphate buffer, 10 mM EDTA at pH 7.0. The dialyzed mAb was then concentrated to 0.5 ml and combined with 0.5 ml of digestion buffer (20 mM cysteine HCl in 20 mM phosphate buffer, 10 mM EDTA, pH 7.0). The solution was then incubated overnight at 37 °C with immobilized papain (Thermo) in a glass tube under gentle agitation. The digested Fab fragment was added to 1.5 ml of 10 mM TRIS buffer, pH 7.5, and the immobilized papain was removed by centrifugation. The digestion mixture was dialyzed for 3 h in the binding buffer (20 mM phosphate buffer, 0.1 M citric acid, pH 7.0) and the Fab fragment was then isolated using a protein A (GE Healthcare) column eluting at 1 ml/min.

2.3. NMR sample preparation and NMR spectroscopy

NMR samples were prepared by dialysis of the lipidated rLP2086-B01 in 30 mM phosphate buffer, 90 mM NaCl containing 1% Zwittergent 3-12 (30 mM) at pH 7.4. The final protein concentration was 0.8 mM. T1, T2 and $^{15}N(^1H)$ NOE relaxation experiments were recorded at a temperature of a 303.15 K, on a Bruker Avance spectrometer operating at Larmor frequencies of 700 MHz and 600 MHz, equipped with triple resonance cryoprobes. All experiments were recorded using standard Bruker pulse sequences. Duplicate T1, T2 and $^{15}N(^1H)$ NOE experiments were recorded with spectral widths of 12,626 Hz and 2199 Hz in the direct (^1H) and indirect (^{15}N) dimensions respectively. For the T1 and T2 experiments, 28 scans were accumulated over 2048 complex points in the ^1H, and 256 complex points in the ^{15}N dimension. Decoupling of ^1H from ^{15}N during acquisition was obtained through a GARP pulse sequence. Relaxation delays between acquisitions were 3 s for the T1 experiments, 6 s for T2, and 3 s for the $^{15}N(^1H)$ NOE experiments. Different T1 experiments were recorded with inversion recovery times of 10, 20, 40, 180, 300, 500, 800, 1300 and 2000 ms. T2 experiments were acquired with delay times of 10, 20, 40, 60, 100, 150, 200 and 350 ms. $^{15}N(^1H)$NOE was measured as difference between two datasets, one recorded with a presaturation period of 3 s using a train of 120 degree proton hard pulses separated by 5 ms intervals, and one with no initial saturation. Saturated and unsaturated spectra were recorded in an interleaved manner.

2.4. Other NMR samples

The spectra of tripalmitoyl-*S*-glycerol-cysteine (Novabiochem) were recorded in $CDCl_3$. The spectra of Zwittergent 3-12 were recorded in phosphate buffer. Assignment of the ^1H resonances for these two compounds was accomplished through 2D $^1H,^1H$ COSY, 2D ^{13}C HMBC and 2D ^{13}C HSQC experiments. NOEs between the lipidated protein, the detergent and the lipid moiety were assigned using a 3D ^{15}N edited NOESY with an ^{15}N-labeled rLP2086-01.

2.5. Data processing and analysis

Data were processed using the NMRPipe suite [12]. R_1 and R_2 relaxation rates and standard deviations were determined by fitting peak intensities with a single exponential decay curve using the built-in function in Sparky [13]. Duplicate experiments were recorded for each mixing time. Error on the peak intensities was calculated as standard deviation of duplicate data points.

Heteronuclear $^{15}N(^1H)$ NOE relaxations were calculated from the ratio of the peak intensities of the saturated to the unsaturated spectra. Standard deviations on the NOE were calculated according to the following formula [14]:

$$\frac{\sigma}{\mathrm{NOE}} = \sqrt{\left(\frac{\sigma I_{\mathrm{SAT}}}{I_{\mathrm{SAT}}}\right)^2 + \left(\frac{\sigma I_{\mathrm{NON-SAT}}}{I_{\mathrm{NON-SAT}}}\right)^2} \quad (1)$$

2.6. Antibody binding by NMR

Binding of Fab fragment to the rP2086-B01 antigen was performed by adding unlabeled MN86-1042-2 Fab to the non-lipidated protein uniformly labeled with ^{15}N and ^{2}H. Two experiments were recorded with protein to Fab fragment ratios of 1:0.5 and 1:1, at 30 °C, and a protein concentration of 200 μM. Identification of the residues involved in antibody interaction was accomplished by identifying peaks experiencing above average intensity reduction or chemical shift perturbation, through two-dimensional ^1H,^{15}N HSQC experiments.

2.7. Flow cytometry

Monoclonal antibodies used in flow cytometry experiments were obtained from mice immunized with rLP2086 variant B01. Bacterial cells were grown to an OD_{650} of 0.45–0.55 and then fixed in 1% paraformaldehyde for 10 min. The bacteria were then plated and washed in 1% BSA/PBS. Following the addition of MN86-1042-2 antibody or 1042-2 Fab fragment, cells were resuspended and added to an ice bath for 30 min. Mouse IgG and MN86-994-11 were used as negative and positive controls, respectively. After two washes in 1% BSA/PBS, biotinylated goat anti-mouse IgG (subclasses 1+2a+2b+3) (Jackson Immunoresearch) or biotinylated anti-mouse IgG (Fab specific) (Sigma) was added to the cells and incubated on ice for 30 min. Cells were washed twice, resuspended in streptavidin–PE (BD Biosciences) and added to an ice bath for an additional 30 min. After two washes in 1% BSA/PBS, the cells were resuspended in 1% paraformaldehyde. Fluorescence intensity was recorded on a Becton Dickinson LSR II flow cytometer and data analyzed with FlowJo version 7 software (Treestar). The mean fluorescence intensity (MFI) of the PE channel was determined for each sample after gating on bacterial cells.

3. Results

3.1. Backbone dynamics

The NMR structure of rLP2086-B01 in micellar solution revealed a novel fold consisting of two domains in contact through two hydrophobic patches [8,9]. The main globular part of the protein is linked to the micelle through a flexible chain (residues 1–20) that anchors the micelle through a tripalmitoyl-*S*-glycerol-cysteine lipid moiety at cysteine 1 (Fig. 1). The folded part of the protein was shown to have no contacts with the micelle. In fact, NOEs between rLP2086-B01 and the micelle are observed only for residues Cys-1 and Gly-2 at the N-terminal chain [8]. NOE assignment between rLP2086-B01, the detergent (Zwittergent 3-12), and the lipid moiety is shown in Fig. 1.

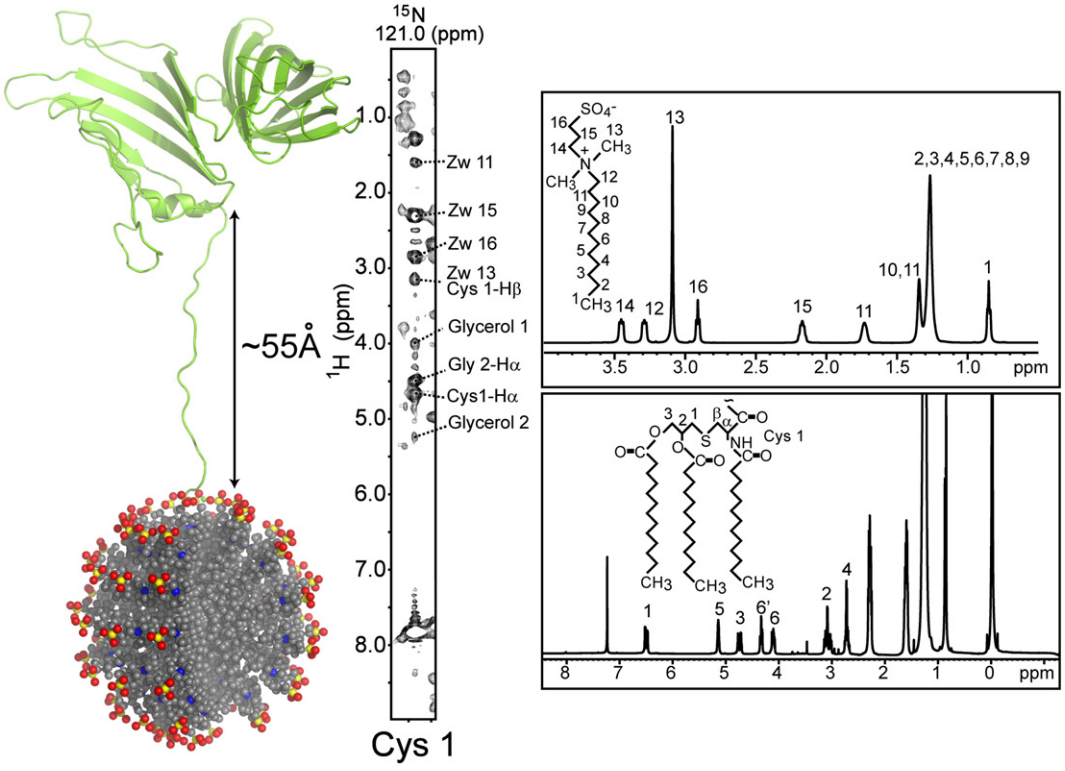

Fig. 1. Graphical representation of LP2086-B01 anchored to a detergent micelle. Left: the 20 residue unstructured chain anchors LP2086-B01 to the surface of a micelle of Zwittergent 3-12 through the tripalmitoyl-*S*-glycerol-cysteine moiety. Based on the length of a fully extended 20 residue polypeptide chain, the unstructured N-terminal is estimated to be able to achieve a maximum length of 55 Å above the micelle. The protein and the detergents were drawn in scale using the program PyMOL [25]. Center: tentative NOE assignments between residue Cys-1, Zwittergent 3-12, and the tripalmitoyl-*S*-glycerol-cysteine from a 3D ^{15}N-NOESY of rLP2086-B01 in micellar solution. Right top: assigned 1D ^1H spectrum of Zwittergent 3-12. Bottom: assigned 1D ^1H spectrum of tripalmitoyl-*S*-glycerol-cysteine.

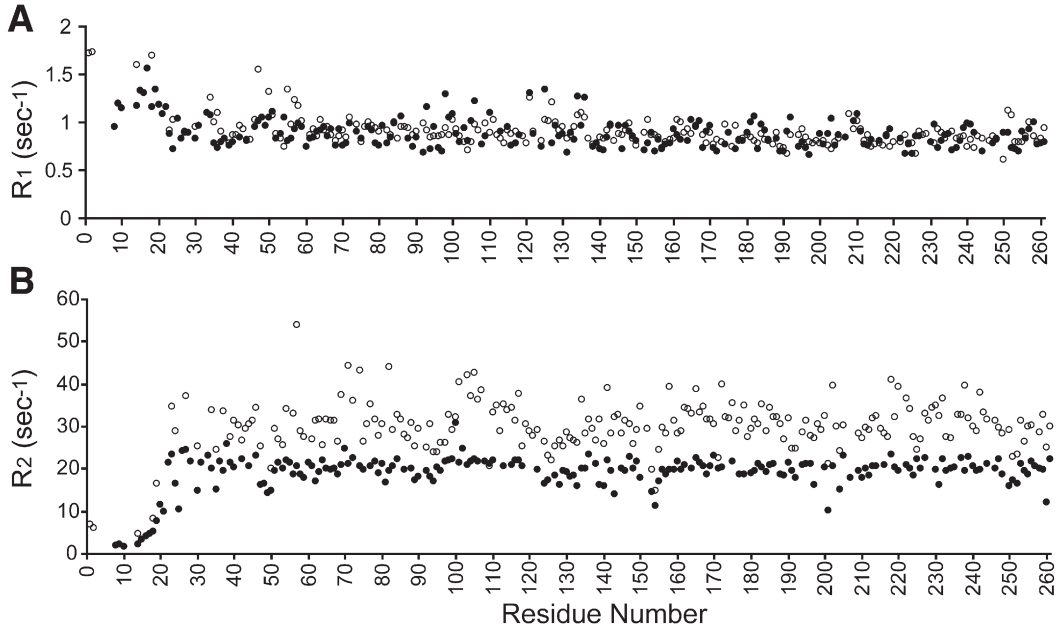

Fig. 2. Longitudinal and transverse relaxation rates of LP2086-B01 measured at 700 MHz. Comparison of (A) longitudinal (R_1) and (B) transverse (R_2) relaxation rates for the non-lipidated protein rP2086-B01 in the absence of detergent (filled circles), and for the lipidated rLP2086-B01 in micellar solution (open circles).

Fig. 2 shows the longitudinal and transverse relaxation rates for LP2086-B01 in both lipidated micellar solution and non-lipidated protein in absence of detergent, measured at 700 MHz. An increase in the transverse relaxation rates R_2 is observed, from an average value of $20.4 \pm 1.3\ s^{-1}$ for the structured part of the non-lipidated protein to $34.1 \pm 6.1\ s^{-1}$ for the lipidated protein in detergent micelle (Fig. 2B). The longitudinal relaxation rates R_1 on the other hand, being less sensitive to increases in correlation times, have comparable values in both conditions (Fig. 2A). The R_2/R_1 ratios and $R_2{*}R_1$ for lipidated LP2086-B01 in micellar solution and for non-lipidated protein in the

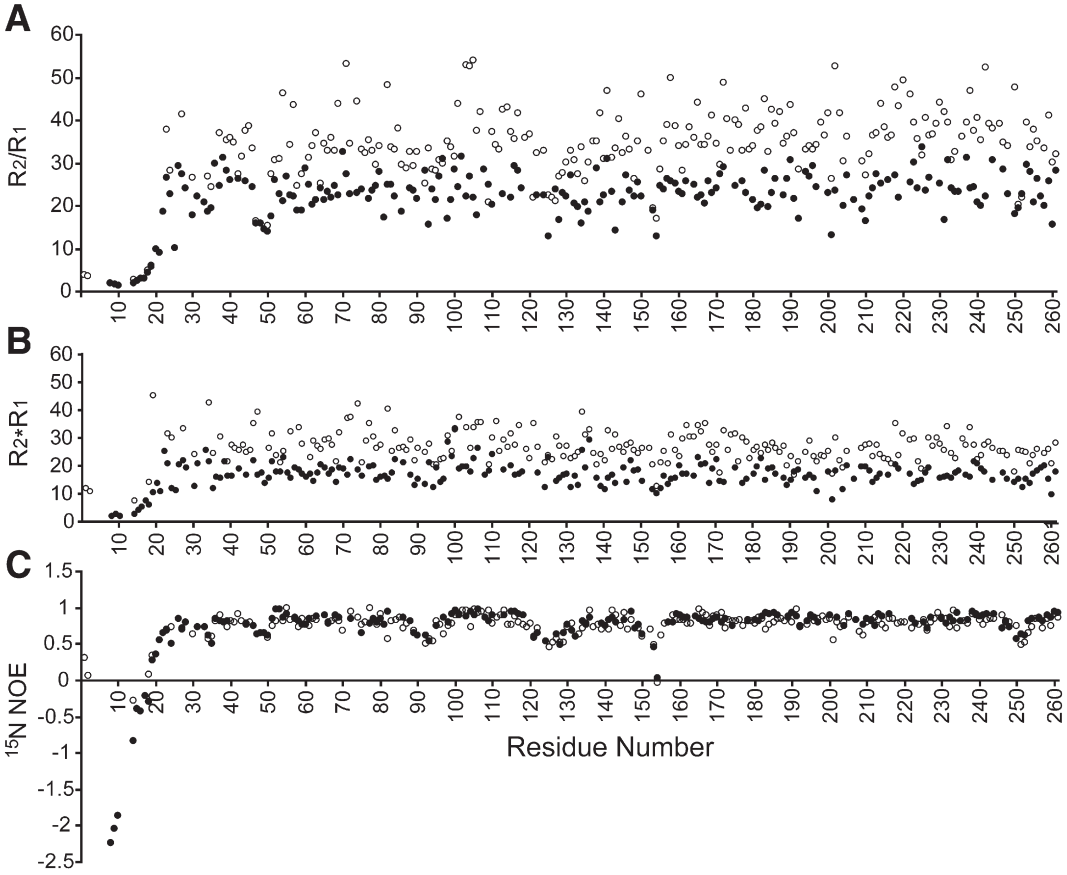

Fig. 3. Backbone dynamics of rLP2086-B01 in micellar and non-micellar samples. (A) R_2/R_1 and (B) R2* R1 values and (C) heteronuclear $^{15}N(^1H)$ NOE for the micelle-bound lipidated rLP2086-B01 in 1% Zwittergent 3-12 (open circles) and for the non-lipidated rP2086-B01 in the absence of detergent (closed circles).

absence of detergent are shown overlaid in Fig. 3A and B, respectively. With the exception of the N-terminal chain and some loops, the values of R_2/R_1 and $R_2{*}R_1$ are uniform across the structured parts of the protein indicating that in both cases, the protein tumbles in solution as a unique globular unit with the two domains moving as one. For the non-lipidated rP2086-B01, the average R_2/R_1 value is 23.8 ± 2.6 for the structured parts of the protein, which is consistent with the molecular weight of the monomeric protein of 27.5 kDa. As evident from Fig. 3A and B, small differences in the average R_2/R_1 and $R_2{*}R_1$ are observable between the non-lipidated protein and the lipidated protein in micellar solution. We observe an increase in the R2/R1 average value for the lipidated rLP2086-B01 in 1% Zwittergent 3-12, to 38.7 ± 8.0.

The N-terminal chain of the lipidated LP-2086-B01 may extend by more than 50 Å above the surface of the micelle, based on the estimated length of a fully extended 20 residue chain. In addition, only NOEs between the first two residues and the micelle were observed, leading us to conclude that the main body of the protein is not in contact with the micelle. This could explain the small differences observed in the R_2/R_1 and $R_2{*}R_1$ values and the corresponding peak widths between the two forms of the protein. Since the aggregation number of Zwittergent 3-12 is 55 (18.5 kDa micelle), the estimated molecular weight of the complex is approximately 46 kDa. Despite the doubling in molecular weight, the peak widths on the 2D ^{1}H,^{15}N-HSQC spectra remained remarkably sharp showing only small increases in line width. The half-height line width for ^{1}H and ^{15}N for the structured parts of the protein increased from average values of 31.2 ± 3.5 Hz (^{1}H) and 11.4 ± 1.1 Hz (^{15}N) for the non-lipidated protein, to 38.7 ± 4.6 Hz (^{1}H) and 12.8 ± 2.0 Hz (^{15}N) for the micelle-bound lipidated protein. These line widths are sharper than what is usually observed for integral membrane proteins of comparable molecular weight in micellar solutions. In fact, the study of membrane proteins by NMR spectroscopy in micellar solutions routinely requires higher temperatures (up to 60 °C) in order to decrease the line widths by increasing the protein tumbling rate in solution [15].

The $^{15}N(^{1}H)$ NOE values measured at 700 MHz for the lipidated and non-lipidated proteins are displayed in Fig. 3C, showing very similar values (within experimental errors) for the two forms of the protein. The average NOE values for the structured parts of the protein are 0.89 ± 0.11 and 0.87 ± 0.08 for the N-domain and the C-domain, respectively. The only exceptions are some of the loops (regions 47–50, 89–96, 121–133, 150–154, and 250–252) which display higher backbone mobility as indicated by their negative or below 0.7 NOE values. Interestingly, the short amphipathic α-helix spanning residues 19–26 has several residues with NOE values below 0.7 indicating that this helix is dynamic in nature. The high flexibility of the N-terminal chain is evidenced by the negative values of $^{15}N(^{1}H)$ NOE as shown in Fig. 3C, with residues Cys-1 and Gly-2 being the exception in the lipidated protein with positive NOE values (0.31 ± 0.01 and 0.07 ± 0.07), in agreement with being buried into the surface of the micelle.

We suggest that the observed increase in R_2 for the lipidated protein arises from steric restrictions imposed by the flexible N-terminal chain anchored to the micelle. Although the free protein in solution can tumble isotropically, the restrain from the N-terminal linker may limit its ability to tumble freely in solution. Interestingly, hydrodynamic calculations conducted with the program Hydronmr [16] produce average values of R_2/R_1 for the free protein of 36.0 ± 3.2 and 26.7 ± 2.4 at 700 and 600 MHz, respectively, which compare well with the experimental values of 38.7 ± 8.0 and 25.8 ± 7.6 observed for rLP2086-B01 in micellar solution. However, the analysis of rLP2086-B01 relaxation data through standard dynamics methodologies based on the model-free approach [17] failed to converge probably due to these unconventional dynamic properties of the protein in complex with the micelle. In contrast to the changes observed in the transverse relaxation rates, the $^{15}N(^{1}H)$ NOE and the R_1 values are virtually identical for the micelle-bound and the free protein in solution, indicating that the presence of the micelle affects the overall tumbling of the whole protein but not the backbone flexibility.

3.2. Epitope mapping with Fab fragment MN86-1042-2

Our interest in confirming the earlier proposed antigen topology in the bacterial membrane [8] led us to perform additional studies of LP-2086-B01 with MN86-1042-2, a subfamily B specific monoclonal antibody. Spectral perturbations such as line broadening or chemical shifts changes are usually observed in the target protein upon interaction with a ligand. For instance, in the case of antigen-Fab interacting with affinities in the μM range, the residues involved in binding can generally be identified by observing differential line broadening upon titration of unlabeled Fab fragment to the ^{15}N labeled antigen [8,18,19]. For antibodies that bind tighter (in the nM-pM range), chemical shift perturbation of uniformly $^{2}H/^{15}N$ labeled antigen and unlabeled Fab fragment can be observed [14,15]. Therefore, residues that are in direct contact with a Fab fragment can be identified by changes observable in a ^{1}H-^{15}N correlation experiment.

Among the pool of monoclonal antibodies identified in our laboratory, we selected MN86-1042-2 due to its specificity to subfamily B of LP2086 and also for its high affinity for the protein. The affinity of MN86-1042-2 to rP2086-B01, as measured from surface plasmon resonance experiments, is ~20 nM (data not shown). Fig. 4A shows the changes observed in the ^{1}H-^{15}N HSQC of perdeuterated ^{15}N labeled rLP2086-B01 in the presence of Fab-1042-2, at ratios of 1:0.5 and 1:1 antigen-Fab. As anticipated, binding with the Fab fragment causes a large reduction in the intensities of the HSQC peaks. However, for several peaks which belong to residues located in the N-domain, an above average reduction in intensity is observed (shown on the surface diagram of LP-2086-B01 in red, Fig. 4B). In addition, peak shifts for other residues also located at the N-domain are observed, which is expected due to the slow exchange between the free and bound forms (shown on the surface diagram of LP-2086-B01 in blue, Fig. 4B). The residues on the N-domain that are affected by the binding of MN86-1042-2 belong to a region of the protein that was previously proposed to be oriented toward the extracellular space [8]. Fig. 4C shows that both MN86-1042-2 monoclonal antibody and MN86-1042-2 Fab fragment can bind equally well to LP2086-B01 on the surface of intact meningococcal B cells, showing that the binding epitope of this antibody is not affected by the presence of the LOS on the outer bacterial surface [8]. Although our data is not sufficient to narrow the specific residues that form the binding epitope of MN86-1042-2, our results clearly indicate that the N-domain is mostly involved in the recognition of MN86-1042-2. In agreement with the NMR binding, competitive flow cytometry experiments using overlapping linear dodecapeptides spanning the entire primary sequence of LP2086-B01 (data not shown) did not identify any peptide that competes for this antibody. This supports the hypothesis that the MN86-1042-2 monoclonal antibody interacts with a conformational epitope spanning a broad region of the protein. In sum, our NMR experiments indicate that the binding of MN86-1042-2 Fab fragment encompasses a large conformational epitope that is extended over a broad region of the N-domain exposed to the extracellular space.

4. Discussion

The ability of surface proteins to elicit bactericidal antibodies depends not only on the intrinsic immunogenic properties encoded in the protein sequence, but also on the accessibility of these binding epitopes to the host immune system. This accessibility can be affected by the presence of other molecular components of the outer bacterial membrane such as the capsule and the layer of lipo-oligosaccharides. The latter were shown to affect the antigenicity of PorB proteins diminishing their efficacy as anti-meningococcal vaccines [5]. The

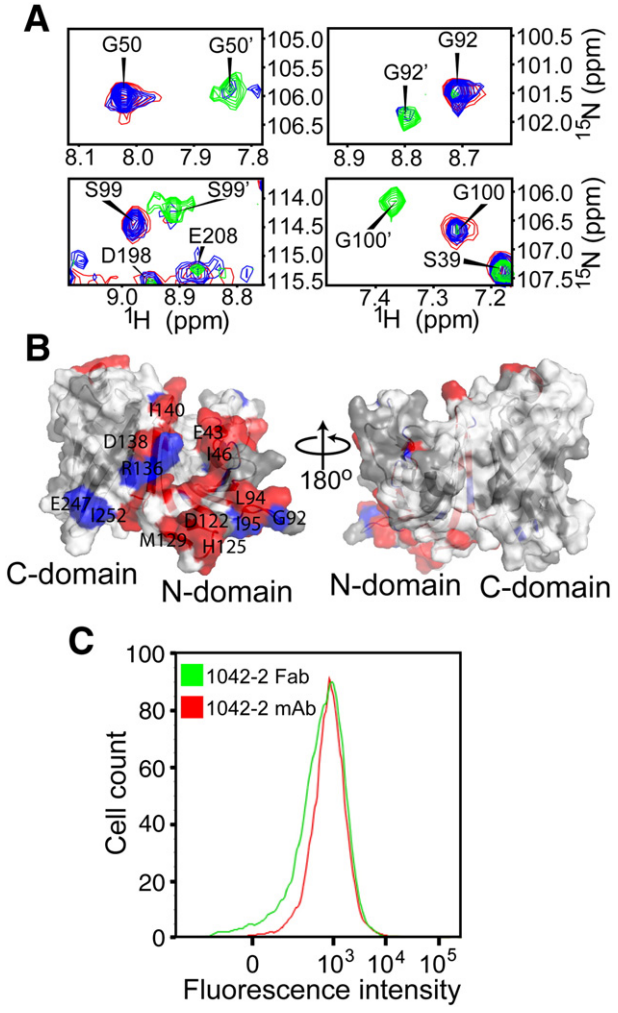

Fig. 4. Binding of a Fab fragment derived from the monoclonal MN86-1042-2 with rP2086-B01. (A) 2D HSQC spectra of representative residues that experience changes upon addition of MN86-1042-2. Free rP2086-B01 (red); rP2086-B01/MN86-1042-2 complex in ratio 1:0.5 (blue); and rP2086-B01/MN86-1042-2 complex in ratio 1:1 (green). (B) Most of the residues affected by the binding with MN86-1042-2 are located on the N-domain. Blue: residues which display peak shifts by more than one line width from the peak of the free protein. Red: residues which peaks that experience above average reduction in signal intensity. Dark gray: unassigned residues due to either exchange with the solvent at pH 7.4 or due to deuteration following the expression of the protein in 99% D_2O. (C) Flow cytometry of Fab fragment derived from the monoclonal MN86-1042-2 (green) and the full-length mAb MN86-1042-2 (red) to MnB show comparable activities.

higher efficacy of the LP2086 family of proteins as vaccine candidate resides in their ability to extend above the layer of lipo-oligosaccharides as shown in the model proposed in Fig. 5A. Very importantly, a recent report indicated that the presence of the capsular polysaccharides does not affect the binding of antibodies directed to LP2086 [22].

The layer of lipo-oligosaccharides, however, may impose additional motional restrictions that limit the protein range of motion above the membrane, while partially shielding one face of the antigen from the antibodies (Fig. 5B). This model would explain the existence of two monoclonal antibodies identified in our laboratories (MN86-813 and MN86-626-15) that recognize the free protein in solution, but do not interact with the membrane bound LP2086 in intact meningococcal cells [8]. For these two mAbs, linear epitopes were identified on one face of the N-domain. On the opposite face of the N-domain, on the other hand, the subfamily B specific monoclonal MN86-1042-2 presented in this work, and two other mAbs (the subfamily B specific MN86-440-18 and the broad spectrum MN86-1075-6) previously studied in our laboratories [8], present overlapping epitopes as shown in Fig. 5A. Since the binding epitopes of these mAbs overlap on the same face of the N-domain, our work further strengthens the importance of the N-domain in antibody recognition, and supports our hypothesis that LP2086-B01 orients one face of the protein toward the host complement system (Fig. 5A).

This model is also in agreement with the recently reported crystal structure of one variant of the LP2086 family in complex with the 6th and 7th domains of human factor H [23]. The structure of the complex reveals that factor H binds rP2086 on the face of the protein exposed to the extracellular space, and its binding surface partially overlaps with the binding epitopes of MN86-1042-2, MN86-440-18 and MN86-1075-6 (Fig. 5A). As revealed by sequence alignment of 172 unique LP2086 sequences, this face of the protein is populated by residues that are responsible for defining the specificity to the two subfamily A and B of serogroup B meningococci [24]. In combination with the observation that monoclonal antibodies against LP2086 mainly display subfamily specific affinities, the presence of an exposed surface of subfamily specific residues can partially explain the immunogenic character of LP2086 [8].

In conclusion, our dynamics data together with binding experiments with the subfamily B specific monoclonal MN86-1042-2 support our previously suggested topological model LP2086-B01 on the outer surface of *N. meningitides*. The degree of exposure of the antigen to the extracellular space is very likely affected by the dynamic properties of the protein when bound to the membrane surface. Membrane bound antigens that are partially immersed in the layer of oligosaccharides could experience a restricted range of motions, thus preventing access of certain epitope regions to the antibody (Fig. 5B). Our dynamics experiments in micellar solution in the absence of the lipo-oligosaccharide layer suggest that even though the lipidated protein is not in direct contact with the micelle, the membrane-bound linker itself seems to induce structural restrictions that affect the protein dynamics which deviate from a fully isotropic tumbling. However, since antibody MN86-1042-2 is still able to bind to the protein, this antigenic face of the LP-2086-B01 is still available, despite the restrictions on protein dynamics imposed by the membrane and the LOS layer. A complete dynamic picture of LP2086-B01 in a realistic membrane mimicking system would require the incorporation of lipo-oligosaccharides in micellar solutions of rLP2086-B01, which would

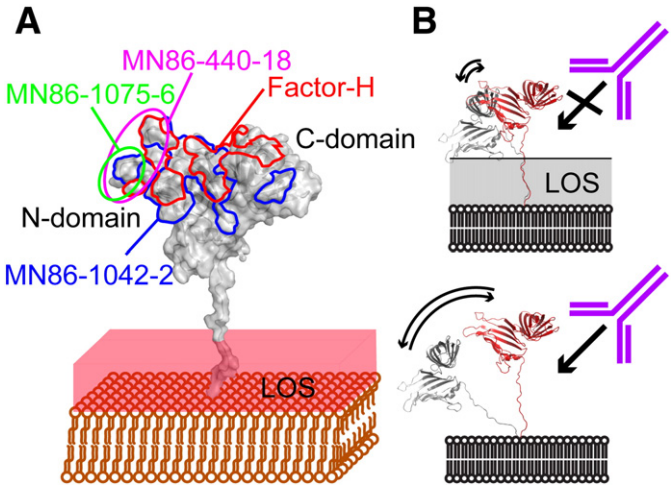

Fig. 5. Dynamic model of LP2086-B01 in the outer bacterial membrane. (A) The surface of interaction with factor H and the binding epitopes for monoclonal antibodies MN86-440-18, MN86-1075-6 and MN86-1042-2 are overlapped and located on one face of the antigen exposed to the extracellular space. (B) The presence of a layer of lipo-oligosaccharides may impose limitations to the dynamics of LP2086-B01, making some epitopes inaccessible by the antibodies. This model is in agreement with the identification of antibodies that recognize the free protein but not the membrane bound LP2086-B01 in whole meningococcal cells [8].

provide a more complete assessment of the degree of restriction that the LOS layer imposes on the protein tumbling and epitope exposure. In fact, it is interesting to consider an extreme scenario where non-covalent interactions between the protein and the LOS could induce a structural change on the N-terminal, thus bringing the antigen in closer proximity to the membrane. Experiments are ongoing in our laboratory to test the effect of the LOS layer on the protein structure and dynamics.

Acknowledgements

We are thankful to Lidia Mosyak and Will Somers for useful discussion on the manuscript. We also thank Amy Tam, May Tam, Wayne Stochaj, Laura Lin, Ron Kriz and Mark Stahl for their support on the experimental work.

References

[1] N. Rosenstein, B. Perkins, D. Stephens, T. Popovic, J. Hughes, Meningococcal disease, N. Engl. J. Med. 344 (2001) 1378–1388.
[2] EU-INS, Invasive *Neisseria meningitidis* in Europe. London: Health Protection Agency; 2006. www.euibis.org.
[3] Centers for Disease Control and Prevention, Active bacterial core surveillance. Atlanta: Centers for Disease Control and Prevention. http://www.cdc.gov/ncidod/dbmd/abcs/meth-surv-pop.htm.
[4] J.T. Poolman, Development of a meningococcal vaccine, Infect agents Dis. 4 (1995) 13–28.
[5] C.L Vermont, H.H. van Dijken, A.J. Kuipers, C.J.P. van Limpt, W.C.M. Keijzers, A. van der Ende, R.d. Groot, L. van Alphen, G.P.J.M. van den Dobbelsteen, Cross-reactivity of antibodies against PorA after vaccination with a Meningococcal B outer membrane vesicle vaccine, Infect. Immun. 71 (2003) 1650–1655.
[6] J. van den Elsen, J.N. Herron, P. Hoogerhout, J. Poolman, E. Boel, T. Logtenberg, J. Wilting, D. Crommelin, J. Kroon, P. Gros, Bactericidal antibody recognition of a PorA epitope of *Neisseria meningitidis*: crystal structure of a Fab fragment in complex with a fluorescein-conjugated peptide, Proteins 29 (1997) 113–125.
[7] A.T. Bentley, P.E. Klebba, Effect of lipopolysaccharide structure on reactivity of antiporin monoclonal antibodies with the bacterial cell surface, J. Bacteriol 170 (1988) 1063–1068.
[8] L.D. Fletcher, L. Bernfield, V. Barniak, J.E. Farley, A. Howell, M. Knauf, P. Ooi, R.P. Smith, P. Weise, M. Wetherell, X. Xie, R. Zagursky, Y. Zhang, G.W. Zlotnick, Vaccine potential of the *Neisseria meningitidis* 2086 lipoprotein, Infect. Immun. 72 (2004) 2088–2100.
[9] S. Pillai, A. Howell, K. Alexander, E.B. Bentley, H.Q. Jiang, K. Ambrose, D. Zhu, G. Zlotnick, Outer membrane protein (OMP) based vaccine for *Neisseria meningitidis* serogroup B, Vaccine 23 (2005) 2206–2209.
[10] A. Mascioni, B. Bentley, R. Camarda, D. Dilts, P. Fink, V. Gusarova, S. Hoiseth, J. Jacob, S. Lin, K. Malakian, L. McNeil, T. Mininni, F. Moy, E. Murphy, E. Novikova, S. Sigethy, Y. Wen, G. Zlotnick, D.H.H. Tsao, Structural basis for the immunogenic properties of the meningococcal vaccine candidate LP2086, J. Biol. Chem. 284 (2009) 8738–8746.
[11] F. Cantini, D. Veggi, S. Dragonetti, S. Savino, M. Scarselli, G. Romagnoli, M. Pizza, L. Banci, R. Rappuoli, Solution structure of the factor H-binding protein, a survival factor and protective antigen of *Neisseria meningitidis*, J. Biol. Chem. 284 (2009) 9022–9026.
[12] F. Porcelli, B.A. Buck-Koehntop, S. Thennarasu, A. Ramamoorthy, G. Veglia, Structures of the dimeric and monomeric variants of magainin antimicrobial peptides (MSI-78 and MSI-594) in micelles and bilayers, determined by NMR spectroscopy, Biochemistry 45 (2006) 5793–5799.
[13] F. Porcelli, R. Verardi, L. Shi, K.A. Henzler-Wildman, A. Ramamoorthy, G. Veglia, NMR structure of the cathelicidin-derived human antimicrobial peptide LL-37 in dodecylphosphocholine micelles, Biochemistry 47 (2008) 557–5565.
[14] F. Delaglio, S. Grzesiek, G.W. Vuister, G. Zhu, J. Pfeifer, A. Bax, , NMRPipe: a multidimensional spectral processing system based on UNIX pipes, J. Biomol. NMR 6 (1995) 277–293.
[15] T. D. Goddard and D. G. Kneller, SPARKY 3, University of California, San Francisco.
[16] N.A. Farrow, R. Muhandiram, A.U. Singer, S.M. Pascal, C.M. Kay, G. Gish, S.E. Shoelson, T. Pawson, J.D. Forman-Kay, L.E. Kay, Backbone dynamics of a free and phosphopeptide-complexed Src homology 2 domain studied by ^{15}N NMR relaxation, Biochemistry 33 (1994) 5984–6003.
[17] B.A. Buck-Koehntop, A. Mascioni, J.J. Buffy, G.J. Veglia, Structure, dynamics, and membrane topology of stannin: a mediator of neuronal cell apoptosis induced by trimethyltin chloride, J. Mol Biol. 354 (1995) 652–665.
[18] J. García de la Torre, M.L. Huertas, B. Carrasco, HYDRONMR: prediction of NMR relaxation of globular proteins from atomic-level structures and hydrodynamic calculations, J. Magn. Reson. B 147 (2000) 138–146.
[19] G. Lipari, A. Szabo, Model-free approach to the interpretation of nuclear magnetic resonance relaxation in macromolecules. 1. Theory and range of validity, J. Am. Chem. Soc. 104 (1982) 4546–4559.
[20] H. Matsuo, K. Walters, K. Teruya, T. Tanaka, G. Gassner, S. Lippard, Y. Kyogoku, G. Wagner, Identification by NMR spectroscopy of residues at contact surfaces in large, slowly exchanging macromolecular complexes, J. Am. Chem. Soc. 121 (1999) 9903–9904.
[21] K. Walters, G. Gassner, S. Lippard, G. Wagner, Structure of the soluble methane monooxygenase regulatory protein B, Proc. Natl. Acad. Sci. 96 (1999) 7877–7882.
[22] X. Huang, X. Yang, B. Luft, S. Koide, Structure-based design of a second-generation Lyme disease vaccine based on a C-terminal fragment of *Borrelia burgdorferi* OspA, J. Mol. Bio. 281 (2005) 61–67.
[23] W. Ding, X. Huang, X. Yang, J. Dunn, B. Luft, S. Koide, C. Lawson, Structural identification of a key protective B-cell epitope in Lyme disease antigen OspA, J. Mol. Bio. 302 (2000) 1153–1164.
[24] L. McNeil, E. Murphy, X. Zhao, S. Guttmann, S. Harris, A. Scott, C. Tan, M. Mack, I. Dasilva, K. Alexander, K. Mason, H. Jiang, D. Zhu, T. Mininni, G. Zlotnick, S. Hoiseth, T. Jones, M. Pride, K. Jansen, A. Anderson, Detection of LP2086 on the cell surface of *Neisseria meningitidis* and its accessibility in the presence of serogroup B capsular polysaccharide, Vaccine 27 (2009) 3417–3421.
[25] M. Schneider, B. Prosser, J. Caesar, E. Kugelberg, S. Li, Q. Zhang, S. Quoraishi, J. Lovett, J. Deane, R. Sim, P. Roversi, S. Johnson, C. Tang, S. Lea, *Neisseria meningitidis* recruits factor H using protein mimicry of host carbohydrates, Nature 458 (2009) 890–893.
[26] E. Murphy, L. Andrew, K. Lee, D. Dilts, K. Ambrose, R. Borrow, J. Findlow, M. Taha, M.A. Deghmane, P. Kriz, M. Musilek, J. Kalmusova, D. Caugant, T. Alvestad, L. Mayer, X. Wang, D. Martin, A. von Gottberg, K. Klugman, A. Anderson, K. Jansen, G. Zlotnick, S. Hoiseth, Sequence diversity of the factor H binding protein vaccine candidate in epidemiologically relevant strains of serogroup B *Neisseria meningitidis*, JID 200 (2009) 379–389.
[27] W. L. DeLano, The PyMOL Molecular Graphics System. 2002. http://www.pymol.org.